ELASTIC LATERAL BUCKLING OF SIMPLY SUPPORTED LITESTEEL BEAMS SUBJECT TO TRANSVERSE LOADING

By Cyrilus Winatama Kurniawan[1] and Mahen Mahendran[2]

ME Research Scholar[1], Professor[2], Faculty of built Environment and Engineering, Queensland University of Technology, Brisbane, Australia

ABSTRACT

The buckling strength of a new cold-formed hollow flange channel section known as LiteSteel beam (LSB) is governed by lateral distortional buckling characterised by simultaneous lateral deflection, twist and web distortion for its intermediate spans. Recent research has developed a modified elastic lateral buckling moment equation to allow for lateral distortional buckling effects. However, it is limited to a uniform moment distribution condition that rarely exists in practice. Transverse loading introduces a non-uniform bending moment distribution, which is also often applied above or below the shear centre (load height). These loading conditions are known to have significant effects on the lateral buckling strength of beams. Many steel design codes have adopted equivalent uniform moment distribution and load height factors to allow for these effects. But they were derived mostly based on data for conventional hot-rolled, doubly symmetric I-beams subject to lateral torsional buckling. The moment distribution and load height effects of transverse loading for LSBs, and the suitability of the current design modification factors to accommodate these effects for LSBs is not known. This paper presents the details of a research study based on finite element analyses on the elastic lateral buckling strength of simply supported LSBs subject to transverse loading. It discusses the suitability of the current steel design code modification factors, and provides suitable recommendations for simply supported LSBs subject to transverse loading.

KEYWORDS

LiteSteel beam, Lateral distortional buckling, Lateral torsional buckling, Transverse loading, Non-uniform moment distribution, and Load height.

1.0 INTRODUCTION

LiteSteel beam (LSB) is a new cold-formed high strength and thin-walled steel section developed by Smorgon Steel Tube Mills, using its patented dual electric resistance welding and automated continuous roll-forming techniques. This section has a unique mono-symmetric channel shape comprising two rectangular hollow flanges and a slender web (Figure 1), and is currently being used as flexural members in the light industrial, commercial and domestic markets. The section depth and flange width of LSB sections vary from 125 to 300 mm (125, 150, 200, 250 and 300) and 45 to 75 mm (45, 60 and 75), respectively. Flange height is one third of flange width for all the sections with their thicknesses varying from 1.6 to 3.0 mm (1.6, 2.0, 2.5 and 3.0). Available LSB sections are identified by the section depth, flange width and thickness, for example, 300x60x2.0LSB (SSTM, 2005). The nominal yield strength of web and flange elements of LSB sections are 380 and 450 MPa, respectively.

Recent research (Mahaarachchi and Mahendran, 2005a) has shown that the structural performance of LSBs for intermediate spans is governed by their lateral distortional buckling (LDB) behaviour as shown in Figure 1(b). Under flexural action, the presence of two stiff hollow flanges and a slender web leads to this buckling mode for which a web distortion occurs in addition to the lateral deflection and twist that occur in the common lateral torsional buckling (LTB) mode (see Figure 1(a)). This therefore reduces its buckling resistance to be lower than that based on lateral torsional buckling. Nevertheless, long span LSBs are governed by LTB mode as for other open steel sections (Figure 1(b)).

Mahaarachchi and Mahendran (2005a) has shown that the modified elastic lateral buckling moment equation developed by Pi and Trahair (1997) to allow for lateral distortional buckling effects can be used adequately for LSB sections. However, this equation is limited to a uniform moment distribution condition that rarely exists in practice (Figure 2). A transverse load on a simply supported beam introduces a non-uniform bending moment distribution, and is also often applied above or below the shear centre (load height effect) as seen in Figure 2. Accurate assessment of these

loading conditions in design is important as they can significantly affect the lateral buckling strength of steel beams.

In the current steel design standards (i.e. Australian, American and British), a simple modification to the elastic lateral buckling moment equation with an equivalent uniform moment factor (moment modification) is used to accommodate the effects of non-uniform moment distribution, while a load height factor is used in the determination of a modified effective length to allow for the effect of loading positions. But they were derived mostly based on the data for conventional hot-rolled, doubly symmetric I-beams subject to lateral torsional buckling. In contrast, LSBs are made of high strength steel and have a unique mono-symmetric cross-section with specific residual stresses and geometrical imperfections along with a unique lateral distortional buckling mode. The moment distribution and load height effects of transverse loading for LSBs, and the suitability of the current steel design code methods to accommodate these effects for LSBs are not yet known. The research study presented in this paper was undertaken to investigate the effects of moment distribution and load height of transverse loading on the lateral buckling strength of simply supported LSBs. Two types of common transverse loading were considered, the uniformly distributed load (UDL) and the mid-span point load (PL) shown in Figure 2. The quarter point loading (QL) was also considered in the moment distribution study. Comparisons with the current steel design code modification factors were also made in order to make suitable recommendations for LSBs subject to transverse loading. This paper presents the details of this study and the results.

2.0 CURRENT DESIGN CODES

Tables 5.6.1 of Australian steel structures design code, AS4100 (SA, 1998), provides the following equivalent uniform moment or moment modification factors (α_m) for beams subject to transverse loading.

$$\alpha_m = 1.13 \text{ for uniformly distributed load} \quad (1a)$$

$$\alpha_m = 1.35 \text{ for mid-span point load} \quad (1b)$$

Alternatively, AS4100 also allows a simple α_m approximation using Equation 2 that applies to any bending moment distribution shown in Figure 3. AS4100 Clause 5.6.3 allows the effect of load height by increasing the effective length with a load height factor of 1.4 in calculating the elastic buckling resistance for top flange loading and 1.0 for bottom flange loading.

$$\alpha_m = \frac{1.7M_m^*}{\sqrt{\left[\left(M_2^*\right)^2 + \left(M_3^*\right)^2 + \left(M_4^*\right)^2\right]}} \leq 2.5 \tag{2}$$

Where

M_m = maximum design bending moment in the segment

M_2, M_4 = design bending moments at the quarter points of the segment and

M_3 = design bending moment at the midpoint of the segment

American steel structures design code, ANSI/AISC 360 (AISC, 2005) provides a general equation of moment modification factor (C_b) as given by Equation 3 for various shapes of bending moment distributions (see Figure 3). This equation was originally developed by Kirby and Nethercot (1979). However, ANSI/AISC 360 does not provide any explicit provision to account for the load height effect.

$$C_b = \frac{12.5M_{\max}}{12.5M_{\max} + 3M_A + 4M_B + 3M_C} \leq 2.27 \tag{3}$$

British steel structures design code, BS5950-1 (BSI, 2000) provides a general equation of moment modification factor (m_{LT}) as given by Equation 4 that is analogous to the AISC equation, which also applies to various shapes of bending moment distributions. The effect of load height when a load is applied at the top flange is included by increasing the effective lengths by 20% (load height factor of 1.2) in calculating the elastic buckling resistance. Otherwise the normal loading condition is assumed.

$$m_{LT} = 0.2 + \frac{0.15M_2 + 0.5M_3 + 0.15M_4}{M_{\max}} \geq 0.44 \tag{4}$$

AS4100, ANSI/AISC 360, and BS5950-1 are hot-rolled steel structural design codes. The cold-formed steel structural design codes generally adopt the equivalent uniform moment factor used in the hot-rolled steel structural design codes although there is limited research in this area. Pi et al. (1998) showed that moment modification factors in AS4100 are reasonably accurate (conservative) for cold-formed channel sections while Pi et al. (1997) demonstrated that they are adequate for cold-formed doubly symmetric hollow flange beams subject to lateral distortional buckling except for beams with low modified slenderness. However, Pi et al. (1999) reported that AS4100 modification factors are not accurate for cold-formed Z-sections. Kitipornchai et al. (1986), Kitipornchai and Wang (1986), Helwig et al. (1997), and Lim et al. (2003) also showed that the accuracy of moment modification factors varied depending on the section geometry of even the hot-rolled sections such as mono-symmetric I-beams and Tee beams.

3.0 FINITE ELEMENT MODELLING OF LSBSs

An elastic finite element (FE) model of LSB was developed using ABAQUS (HKS, 2005), which was a modification of the earlier model developed by Mahaarachchi and Mahendran (2005a). It accounts for various LSB buckling deformations, i.e. local, lateral and torsional buckling, and web distortion. ABAQUS S4R5 shell element was selected for the finite element model of LSB as it is capable of providing sufficient degrees of freedom to explicitly model buckling deformations. This element is a thin, shear flexible, isoparametric quadrilateral shell with four nodes and five degrees of freedom per node, utilizing reduced integration and bilinear interpolation schemes. An element size of 5 mm laterally for both the flanges and web of LSB with length in the longitudinal direction of 10 mm was used to provide adequate accuracy (Figure 4). Figure 5 shows the boundary conditions used to simulate the required simply supported condition. A simply supported condition was defined as both ends fixed against vertical deflection, out-of plane deflection and twist rotation, but unrestrained against in-plane rotation, minor axis rotation, warping displacement, while only one end is fixed against longitudinal horizontal displacement. The pin support (at one end) was modelled by using a single point constraint (SPC) of “1234” applied to the node at the middle of the web element, while the degrees of freedom “234” of the other

nodes were restrained. To simulate the roller support at the other end, all the nodes degrees of freedom “234” were restrained. The degrees of freedom notation “123” corresponds to translations in x, y and z axes whereas “456” relates to rotations about x, y and z axes, respectively.

Two types of loading conditions were simulated, equal end moments, and transverse loading. The first loading condition was used as the basic case of uniform moment to demonstrate the moment distribution effect, while in the second loading condition, transverse loads were applied to the top flange, the shear centre and the bottom flange to simulate the load height effect (see Figure 2). The end moment was simulated with linear forces applied at every node of the beam end, where the upper part of the section was subject to compressive forces while the lower part was subject to tensile forces as shown in Figure 5.

A simulation of transverse loading at the shear centre (located away from the cross section) in three dimensional modelling using shell elements is complex and difficult to achieve. Hence an approximate method was adopted to simulate the shear centre loading as shown in Figure 6. In this method, transverse loads (P) were applied to the web elements of LSB’s top and bottom hollow flanges while lateral forces (P’) were applied through the nodes at the corners of the outer flange plate element and the web element of LSB hollow flanges (both top and bottom flanges). The lateral forces (P’) created a torque to counter the torque caused by the loading away from the shear centre. This approach provided an equivalent loading condition to the ideal shear centre loading. Further, the transverse loads were distributed to the web element of LSB’s hollow flanges to reduce possible stress concentrations. The same modelling approach was used to simulate the load height effects as shown in Figure 7. The transverse loads on the web element of LSB’s bottom flange was simply removed to simulate the top flange loading while the removal of transverse loads on the web element of LSB’s top flange simulated the bottom flange loading. Note that the lateral forces (P’) were also applied to provide the required counter torque (see Figure 7).

A series of elastic buckling analysis was carried out to obtain the elastic lateral buckling moments (LDB and LTB) of simply supported LSBs subject to moment distribution and load height effects of transverse loading. Elastic buckling behaviour

of three LSB sections was investigated to include the effect of section geometry in the investigation, LSB125x45x2.0, LSB250x60x2.0 and LSB300x75x3.0. Based on AS4100 rules, they are classified as compact, non-compact and slender sections, respectively. The beam lengths were varied from intermediate to long spans to observe the relationship of lateral buckling modes (LDB vs. LTB) to the loading conditions.

4.0 VALIDATION OF THE FINITE ELEMENT MODEL

The developed finite element model of LSB was able to simulate the three distinct buckling modes of local buckling for short spans, lateral distortional buckling for intermediate spans and lateral torsional buckling for long spans. To verify the accuracy of the adopted finite element type, mesh density, loading (the basic uniform moment case) and boundary conditions, the solutions of the elastic buckling analyses using the finite element model for LSBs subject to a uniform moment were compared with the solutions obtained from finite strip analyses based on THINWALL (Hancock and Papangelis, 1994), and the modified elastic lateral buckling moment equation developed by Pi and Trahair (1997), which allows for the lateral distortional buckling effects as follows.

$$M_{od} = \sqrt{\frac{\pi^2 EI_y}{L^2}\left[GJ_e + \frac{\pi^2 EI_w}{L^2}\right]} \tag{5a}$$

Where the approximate effective torsional rigidity (GJ_e) is given by:

$$GJ_e = \frac{2GJ_F \dfrac{Et^3L^2}{0.91\pi^2 d_1}}{2GJ_F + \dfrac{Et^3L^2}{0.91\pi^2 d_1}} \tag{5b}$$

EI_y = minor axis flexural rigidity

EI_w = warping rigidity

J_F = torsion constant for a single hollow flange

d_1 = depth of the flat portion of the web

t = thickness

L = beam length

Figure 8 compares the elastic buckling moments versus span results obtained from the three methods. It shows that finite element analysis (FEA) results agree well with the results from both THINWALL and M_{od} equation, with an average difference of less than 2% and 3%, respectively. For short span LSBs, both FEA and THINWALL predicted local buckling as the critical buckling mode (precedes lateral distortional buckling). LSB250x60x2.0 and LSB300x75x3.0 appear to be subjected to local buckling when the span is between 1.0 and 1.5m or less while for LSB125x45x2.0 the relevant span is between 0.3 and 0.75m or less. The elastic lateral distortional buckling moment can be obtained from THINWALL for short span LSBs, but this was not feasible in FEA. Therefore it was also not possible to use FEA to investigate the moment distribution effect for the full range of beam slenderness of LSBs (only feasible for intermediate to long spans). Nevertheless, these comparisons indicate that the adopted finite element model is sufficient to predict the elastic buckling moments for all the buckling modes associated with LSB sections, i.e. local buckling, lateral distortional buckling and lateral torsional buckling modes.

5.0 FINITE ELEMENT ANALYSIS RESULTS AND DISCUSSIONS

5.1 Non-uniform Moment Distribution Effect of Transverse Loading

Tables 1 and 2 present the elastic buckling moment results for simply supported LSBs subject to transverse loads (the uniformly distributed load (UDL) and the mid-span point load (PL)) at the shear centre. The equivalent uniform moment distribution factors (α_m) are also presented in Tables 1 and 2. The factor α_m is the ratio of the elastic lateral buckling moments for non-uniform moment ($M_{od\text{-}non}$) and uniform moment (M_{od}) conditions, i.e. $\alpha_m = M_{od\text{-}non} / M_{od}$. The elastic lateral distortional buckling moment given by Equation 5a can be written as:

$$M_{od} = \sqrt{\frac{\pi^2 EI_y GJ_e}{L^2}\left(1 + K_e\right)} \qquad (6a)$$

where;

$$K_e = \sqrt{\pi^2 EI_w / GJ_e L^2} \qquad (6b)$$

K_e is a modified torsion parameter which expresses not only the torsion component of lateral buckling, but also the web distortion. Low K_e value means high beam slenderness and vice versa. In comparison to lateral torsional buckling, the above equations use the effective torsional rigidity parameter GJ_e instead of GJ.

The results in Tables 1 and 2 are also plotted against the modified torsion parameter (K_e) in Figures 9 and 10, respectively. The results generally show that the non-uniform moment distribution caused by transverse loading increases the elastic lateral buckling strength of simply supported LSBs compared with the uniform moment case. The mid-span point load (PL) case provides higher strength benefits because of less severe moment distribution than in the uniformly distributed load (UDL) case, i.e. high moment region is concentrated at mid-span. However a variation of non-uniform moment benefits exists for both UDL and PL cases as shown in Figures 9 and 10 where the α_m factors appear to be a function of the modified torsion parameter (K_e). The α_m factors reach the upper bound for LSBs with high beam slenderness (lower K_e values) where they are subjected to lateral torsional buckling, but they progressively reduce with increasing K_e values (lower beam slenderness) along with increasing level of web distortion during lateral buckling, ie. lateral distortional buckling. This may indicate that the lateral distortional buckling mode unfavourably influences the non-uniform moment distribution benefits, more importantly when the web distortion is significant.

The α_m factor variation also demonstrates that it is more severe for LSBs with transverse loading compared to the moment gradient case. This may be because unlike for LSBs subject to a moment gradient, shear stresses are not negligible for the transverse loading cases, which appear to increase the reduction of non-uniform moment benefits due to the web distortion effect of LDB. A study by Ma and Hughes (1996) also showed the significant effects of uniformly distributed vertical load on the lateral distortional buckling strength of monosymmetric I-beams in comparison to the uniform moment case.

Figures 9 and 10 compare the α_m factors based on FEA results and AS4100 (Eq.1a, 1b and 2), ANSI/AISC 360 (Eq.3) and BS5950-1 (Eq.4). They indicate that the current steel design code factors do not provide accurate predictions. It is evident that the current α_m factors are unconservative as they are given as constant values (i.e. 1.13 for UDL and 1.35 for PL based on AS4100 Table 5.6.1), independent of beam and section slenderness. This does not reflect the observed α_m variation due to web distortion. The comparison also shows that the specific factors in Table 5.6.1 of AS4100 (Eq.1a and 1b) are closer to the upper bound results, implying that it may only be suitable for LSBs subjected to lateral torsional buckling. This observation is justifiable as this α_m equation was originally developed for lateral torsional buckling.

The FEA results also show that LSBs with higher K_e values may be subject to other buckling modes which precede lateral distortional buckling mode. For the UDL case, this non-lateral buckling mode is shear buckling near both supports, and for the PL case it is a local web buckling (or web bearing buckling) at mid-span. This is because the transverse loading is always accompanied by shear stresses which become more critical than the bending stresses in the case of low beam slenderness. When the bending stresses are dominant, the shear stresses can be negligible such as in the intermediate and high beam slenderness cases. Further, a transition mode occurs ($K_e \geq$ 0.8 approximately) from pure lateral buckling mode to the non-lateral buckling mode, which appears to be an interaction of the two buckling modes. Figures 11 (a) to (e) show these non-lateral buckling modes of LSBs with higher K_e values (lower beam slenderness). As the purpose of α_m factor is for the pure lateral buckling (LDB and LTB), such results that were limited by other buckling modes (including interaction) are not relevant and thus were not considered in this study. Elastic buckling analysis based on the three dimensional shell finite element models was not able to provide the lateral buckling moments for the full beam slenderness range of LSBs. Thus if required, other elastic buckling analysis techniques such as energy methods may have to be used to derive solutions exclusively for lateral distortional buckling, especially for cases with higher K_e values.

The variation of α_m factor as shown in Figures 9 and 10 is quite interesting as it appears to keep decreasing with increasing K_e value, where at one stage (higher K_e

values) it may become less than one (i.e. LSB's lateral buckling strength is below that of the basic uniform moment case). However, this is due to the presence of non-lateral buckling modes in the region of low beam slenderness, which suggests that the α_m factor should not be less than one. Also at that stage, it is close to the local buckling region based on the results from the basic case of uniform moment (Figure 12), where the moment distribution effect is negligible. A comparison of elastic buckling moments for transverse loading and uniform moment cases in Figure 12 shows why the α_m factor decreases in this region of low beam slenderness.

A more accurate α_m factor for both UDL and PL cases than the currently available factors can be obtained by developing an equation as a function of K_e to reflect the level of web distortion of LDB and assuming the lower bound of α_m factor as 1.0.

For UDL: $\alpha_m = 1.125 - 0.145\ K_e^2 + 0.008\ K_e \quad (1.0 \leq \alpha_m \leq 1.125)$ (7a)

For PL: $\alpha_m = 1.34 - 0.25\ K_e^2 + 0.06\ K_e \quad (1.0 \leq \alpha_m \leq 1.34)$ (7b)

These equations were derived based on the best fit of data associated only with lateral buckling (LDB and LTB) in Figures 9 and 10 with an average percentage error less than 1%. They appear to be more complex, requiring the calculation of the modified torsion parameter (K_e). However, it is considered as simple to use since all the required parameters in the calculation of K_e are readily available in the Design Capacity Tables of LSBs (SSTM, 2005).

Finite element analyses were also conducted for simply supported LSBs subjected to quarter point loads (QL) and the elastic buckling moment results were analysed using the same procedure as described above for the other two transverse load cases. The results showed that the benefits for the QL case are very small for LSBs. The highest α_m factor was found to be 1.04 (4% improvement from the basic case of uniform moment), which was obtained for LSBs subject to LTB. This is because the bending moment distribution for the QL case is closer to a uniform moment distribution, thus only a negligible benefit will result. As for the other two transverse load cases, the level of web distortion in LDB mode was also found to be unfavourable to the already

small strength benefits for the QL case. As in the other two transverse load cases, it is reasonable to ignore the moment distribution effect for LSBs subjected to non-lateral buckling modes as well as the interaction buckling mode that occur with increasing K_e values. It appears that completely neglecting the benefits for QL is an ideal solution as it is not worth increasing the design complexity for a small moment capacity gain at the most. Comparison with the currently used α_m factors generally agree with this recommendation as they (Equations 2, 3 and 4) also recommend an α_m factor equal to 1.0, except for the factor given in AS4100 Table 5.6.1 (α_m = 1.09). The factor in Table 5.6.1 of AS4100 is unconservative and is not even close to the FEA results of the case subjected to LTB mode. Hence the use of this higher α_m factor of 1.09 is not suitable for LSBs. Nevertheless, if a more accurate prediction is required, then the following α_m equation can be used to take into account the benefits from QL with an assumption that α_m shall not be less than one.

For QL: $\alpha_m = 1.04 - 0.22\, K_e^2 + 0.025\, K_e \qquad (1.0 \le \alpha_m \le 1.04)$ (7c)

On the use of α_m or C_b factors to determine the design moment capacities of LSBs, it is recommended that the design method in many cold-formed steel codes is used in which the elastic lateral buckling moment for the uniform moment case is modified by using the appropriate α_m or C_b factor and used in the member capacity calculation.

5.2 Load Height Effect of Transverse Loading

The load height effect was studied for simply supported LSBs subject to the first two transverse load cases of uniformly distributed load and mid-span point load at the top flange (TF) and bottom flange (BF) loading discussed in the last section. Table 3 presents the elastic buckling moment results from the finite element analyses. The results are also presented in a dimensionless format in Figure 13 where the dimensionless buckling load (DBL) is defined as follows:

For UDL: $DBL = QL^3 / \sqrt{EI_y GJ_e}$ (8a)

For PL: $DBL = QL^2 / \sqrt{EI_y GJ_e}$ (8b)

where the buckling load (Q) is obtained from the elastic buckling finite element analysis and L is the span.

Figure 13 demonstrates that the destabilising effect of loading above the shear centre (top flange loading) decreases the buckling resistance while the loading below the shear centre (bottom flange loading) produces the opposite effect. When a transverse load acts above the shear centre and moves with the beam during lateral buckling, it exerts an additional torque about the shear centre axis, subjecting the section to an additional twisting thus reducing the buckling resistance. Conversely, for loading below the shear centre, the additional torque opposes the twist rotation of the beam, thus increasing the buckling resistance. Figure 14 shows the differences in the torsion level of LDB for various load heights (shear centre, top flange and bottom flange). This effect is more important for beams with low beam slenderness as the torsion level is significant to create a larger additional torque than for beams with higher beam slenderness for which its lateral component is more dominant than the torsion components. This is evident from the results that the load height effect is more important for LSBs with a high modified torsion parameter (K_e). However, the elastic buckling analyses for cases with high K_e values were also limited by other buckling modes which precede lateral distortional buckling (similar to the moment distribution study). The results associated with non-lateral buckling modes were therefore not considered in this study on load height effects.

BS5950-1 (BSI, 2000) and AS4100 (SA, 1998) treat the destabilising effect of top flange (TF) loading by using a factor known as load height factor (k_l) to increase the effective length ($L_e = L \times k_l$). They recommend k_l factors of 1.4 and 1.2, respectively, for this purpose. The increased effective length can be used to calculate the elastic buckling resistance ($M_{od\text{-}non}$) for top flange loading using Equations 5 (a) and (b). However for loading below the shear centre (i.e. BF loading), both design codes conservatively ignore its beneficial effects. The British cold-formed steel design code, BS5950-5 (BSI, 1998) adopts a similar load height factor as in BS5950-1. However, other cold-formed steel design codes, AS/NZ4600 (SA, 2005) and AISI Specification (AISI, 2004), do not provide any explicit provisions to take account of load height effect.

Figures 15 and 16 compare the dimensionless buckling loads from the elastic finite element buckling analysis results with the predictions using BS5950-1 and AS4100 for top flange loading. In calculating the $M_{od\text{-}non}$ for top flange loading using the design code method of effective length, the actual α_m factors based on the elastic buckling analyses in the previous section were used to include the moment distribution effects, ie. the final $M_{od\text{-}non}$ value was obtained by multiplying the $M_{od\text{-}non}$ value from Eq.5a based on the increased effective length with the actual α_m factor. The comparison indicates that the design code prediction does not represent the actual load height effect (TF) variation, i.e. too conservative for lower K_e value (higher beam slenderness) and unconservative for the opposite case, particularly with BS5950-1 predictions. AS4100 prediction is better than that of BS5950-1 as it is only slightly unconservative in the higher K_e region due to its higher load height factor (k_l) of 1.4 (1.2 in BS5950-1).

Trahair (1993) provides an approximate solution to predict the elastic lateral buckling strength of a beam subjected to load height effects as given by the following equation.

$$\frac{M_{cr}}{M_{yz}} = \alpha_m \left\{ \sqrt{\left[1 + \left(\frac{0.4\alpha_m y_Q}{M_{yz}/P_y} \right)^2 \right]} + \frac{0.4\alpha_m y_Q}{M_{yz}/P_y} \right\} \qquad (9)$$

Where; M_{cr} = elastic lateral buckling moment including load height effect

M_{yz} = elastic lateral buckling moment for uniform moment case (M_{od})

y_Q = load height

P_y = $\pi^2 E I_y / L^2$

The use of this more accurate equation for design purposes is permitted in AS4100 (SA, 1998). Figures 15 and 16 also plot the dimensionless buckling load (DBL) calculated using Trahair's solution. In using Equation 9, actual α_m factors based on the elastic buckling analyses presented in the previous section were used to include the moment distribution effect. The comparison demonstrates that Trahair's equation is reasonably accurate with the elastic buckling results for both TF and BF cases. Thus this equation can be safely implemented to calculate the LSB's lateral buckling

moments (LDB and LTB), provided an appropriate α_m factor is used. The use of accurate α_m factors, which include the unfavourable effect of web distortion in lateral distortional buckling, allows treating the load height effects without considering the web distortion effect. In other words, the web distortion effect is exclusively considered within the moment distribution effects. Note that accurate α_m factors are also used in the comparisons using BS5950-1 and AS4100.

Trahair's equation appears to be superior than the current design method based on effective length concept as it can be applied for any load heights using the y_Q parameter in Equation 9 (not limited to TF and BF cases). The comparison of predictions from Trahair's equation and AS4100 for the TF case in Figures 15 and 16 indicates that for LSBs with lower beam slenderness (higher K_e value), they are quite close although the latter is less accurate (slightly unconservative). The slight overestimation from AS4100 method may not be very significant for design purposes as there are many other unaccounted factors that may compensate for this inaccuracy. The effective length method is also easier to use than Equation 9 due to its simplicity and conservatism for cases with high beam slenderness. Therefore the use of AS4100 method based on effective length may be still adequate for LSBs.

The current steel design codes usually ignore the beneficial effects of loading below the shear centre. Its significant benefits are not important, particularly for intermediate and short spans as its ultimate strength is very likely to be limited by its section capacity, while unrestrained long span beams are rarely used in practice. This conservative approach can be safely adopted for LSB design. Alternatively, Trahair's equation (Eq. 9) can be simply used to obtain the higher elastic buckling moment (M_{cr}) for loading below the shear centre of LSBs.

Further, the load height effects due to TF and BF loading can also be expressed as a load height ratio, which is defined as the ratio of elastic lateral buckling moment for the case of top or bottom flange loading to that for shear centre loading. Figure 17 uses this format and plots the elastic buckling analysis results from this study as well as the predictions based on the current design code methods and Trahair's equation (Eq. 9). It is therefore able to confirm the many observations made based on Figures

15 and 16. It also demonstrates that the variation between the two transverse load cases (PL and UDL) can be considered small, indicating that these two cases are sufficient to represent the load height effect on LSBs, although further research into other transverse load types may be useful.

6.0 CONCLUSIONS

This paper has described a series of finite element analyses undertaken to investigate the moment distribution and load height effects of transverse loading on the elastic lateral torsional and distortional buckling strength of simply supported LSBs. The strength benefit due to non-uniform moment distribution reaches the upper bound for LSBs with high beam slenderness, but it reduces with lower beam slenderness due to the increasing level of web distortion of lateral distortional buckling as well as increasing shear stresses, until other buckling modes that precede lateral buckling govern. The current moment distribution (α_m) factors in AS4100, ANSI/AISC 360 and BS5950-1 were found to be inadequate. Hence it is recommended that the new α_m equations proposed in this paper are used in the design of LSB flexural members. The effect of loading above the shear centre creates additional twisting that reduces the elastic lateral buckling resistance of simply supported LSBs, while loading below the shear centre produces the opposite effects. The benefit of the latter is often neglected in the current steel design codes, and the same approach can also be conservatively used for LSBs. For top flange loading, the approximate AS4100 method based on an increased effective length is reasonably adequate to allow for its destabilising effects. A more accurate method is also given in this paper to calculate the elastic lateral buckling moments of LSBs with any load height. The proposed α_m equations incorporate the unfavourable effect of web distortion, thus its use is also important for the accurate assessment of load height effects on simply supported LSBs subject to transverse loading.

7.0 ACKNOWLEDGEMENT

The authors wish to thank Queensland University of Technology, Australian Research Council and Smorgon Steel Tube Mills for supporting this research project.

8.0 REFERENCES

American Institute of Steel Construction (AISC) (2005), ANSI/AISC 360-05 *Specification for Structural Buildings*. Chicago, USA

American Iron and Steel Institute (AISI) (2004), Specification for the Design of Cold-Formed Steel Structural Members, American Iron and Steel Institute, Washington D.C., USA.

British Standards Institution (BSI) (2000), BS5950-1 Structural Use of Steelwork in Buildings – Part1, Code of Practice for Design Rolled and Welded Sections, England.

British Standards Institution (BSI) (1998), BS5950-5 Structural Use of Steelwork in Buildings – Part5, Code of Practice for Design of Cold Formed Thin Gauge Sections. England.

Hancock, G. J. and Papangelis, J.P. (1994), *THINWALL User Manual*, Centre for Advanced Structural Engineering, University of Sydney, Sydney, Australia.

Helwig, T. A., Frank, K. H. and Yura, J. A. (1997), 'Lateral-torsional Buckling of Singly Symmetric I-beams', *Journal of Structural Engineering*, 123(9): 1172-1179.

Hibbitt, Karlsson and Sorensen (HKS) (2005), *Abaqus User Manual*, Pawtucket, RI, USA.

Kirby, P. A. and Nethercot, D. A. (1985), *Design for Structural Stability*, William Collins Sons & Co Ltd, London, UK.

Kitipornchai, S., Wang, C.M. and Trahair, N. S. (1986), 'Buckling of Monosymmetric I-beams under Moment Gradient', *Journal of Structural Engineering*, 112(4): 781-799.

Kitipornchai, S., and Wang, C. M. (1986), 'Lateral Buckling of Tee Beams under Moment Gradient', *Computers & Structures*, 23(1): 69-76.

Lim, N.-H., Park, N.-H., Kang, Y.-J. and Sung, I.-H. (2003), 'Elastic buckling of I-beams under linear moment gradient', *International Journal of Solids and Structures*, 40(21): 5635-5647.

Ma, M. and Hughes, O. (1996), 'Lateral Distortional Buckling of Monosymmetric I-beams under Distributed Vertical Load', *Thin-Walled Structures*, 26(2): 123-145.

Mahaarachchi, D. and Mahendran, M. (2005a), *Finite Element Analysis of LiteSteel Beam Sections,* Research Report No.3, Queensland University of Technology, Brisbane, Australia.

Mahaarachchi, D. and Mahendran, M. (2005b), *Moment Capacity and Design of LiteSteel Beam Sections.* Research Report No.4, Queensland University of Technology, Brisbane, Australia.

Pi, Y.-L. and Trahair, N. S. (1997), 'Lateral-distortional buckling of hollow flange beams', *Journal of Structural Engineering*, 123(6): 695-702.

Pi, Y.-L., Put, B. M. and Trahair, N. S. (1998), 'Lateral Buckling Strengths of Cold-formed Channel Section Beams*', Journal of Structural Engineering*, 124(10): 1182-1191.

Pi, Y.-L. Put, B. M. and Trahair, N. S. (1999), 'Lateral Buckling Strengths of Cold-formed Z-section Beams', *Thin-Walled Structures*, 34(1): 65-93.

Smorgon Steel Tube Mills (SSTM) (2005), *Design Capacity Tables for LiteSteel Beams,* Smorgon Steel Tube Mills, Brisbane, Australia.

Standards Australia (SA) (1998), AS 4100 *Steel Structures*, Sydney, Australia.

Standards Australia (SA) (2005), AS/NZS 4600 *Cold Formed Steel Structures*. Sydney, Australia.

Trahair, N. S. (1993), *Flexural-Torsional Buckling of Structures*, 1st Edition, Chapman & Hall, London, UK.

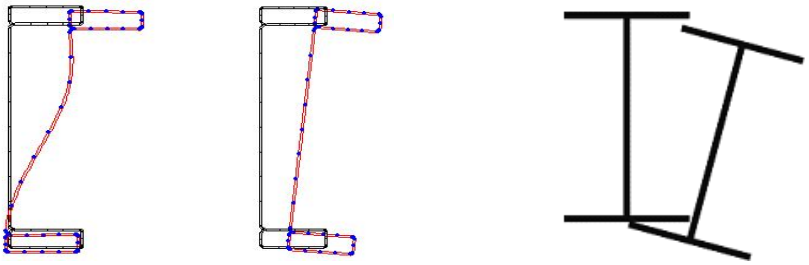

(a) LiteSteel Beams (LDB and LTB) (b) I-beams (LTB)

Figure 1: Lateral Buckling Modes of Beams

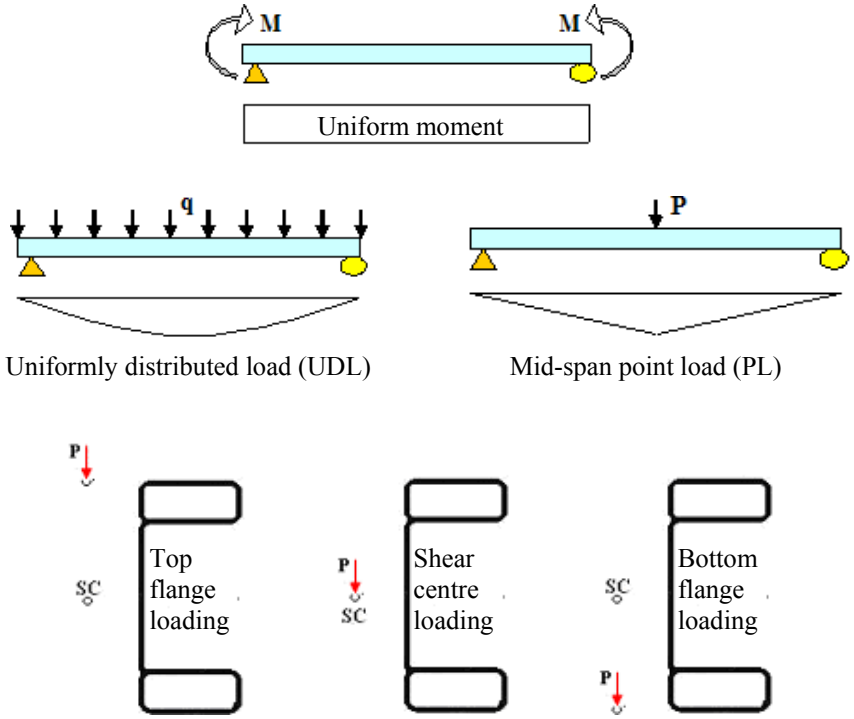

Figure 2: Simply Supported Beam with Various Loading Conditions

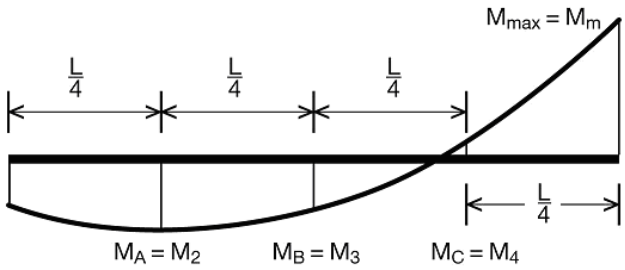

Figure 3: Moment Diagram for Equations (1) to (4)

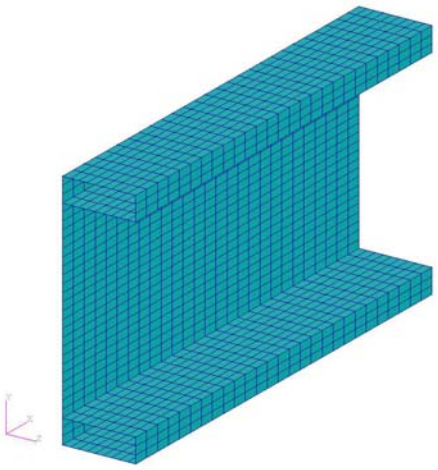

Figure 4: Typical Finite Element Mesh for LSB Model

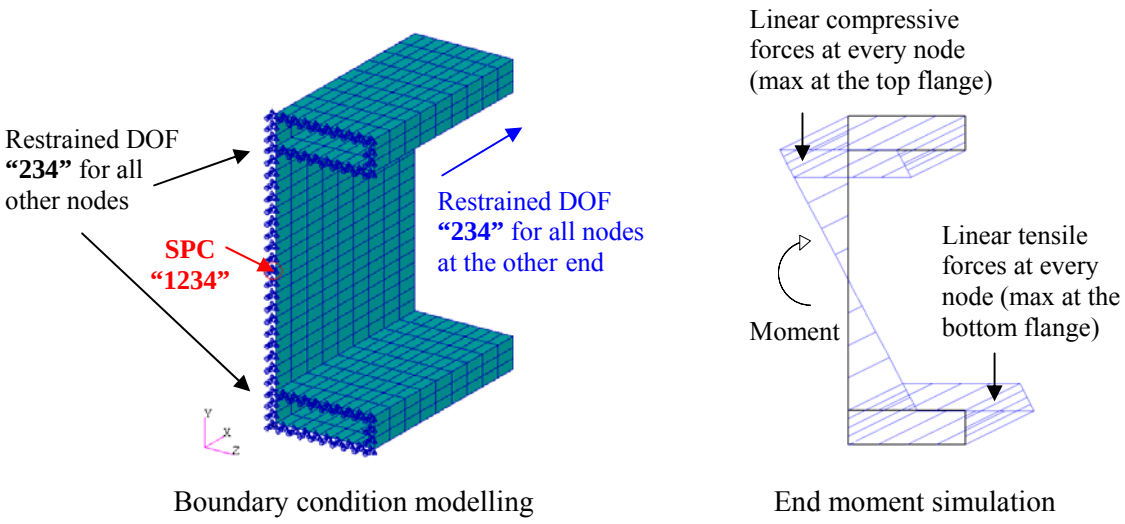

Figure 5: Modelling of Boundary Conditions and End Moment

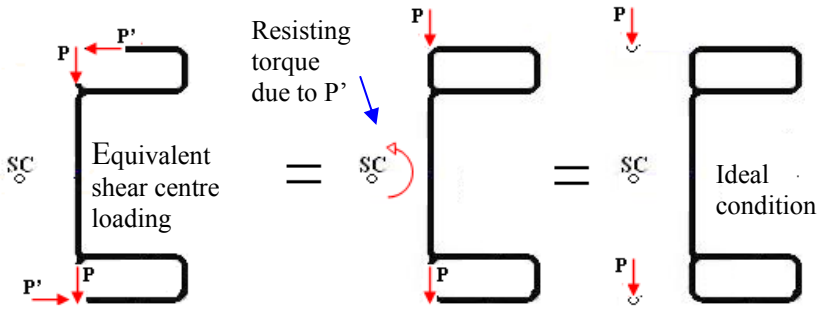

Figure 6: Schematic View of Modelling Transverse Load at Shear Centre

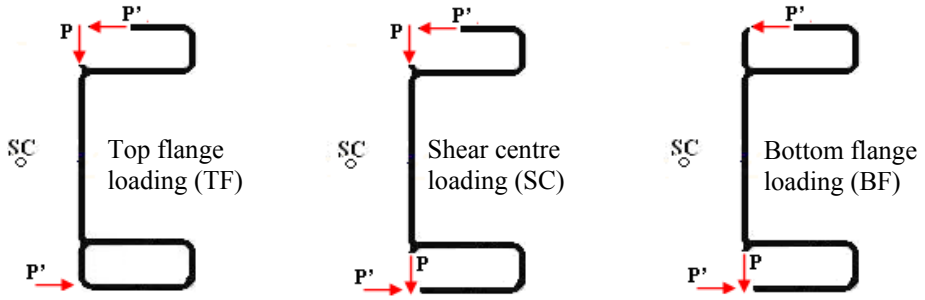

Figure 7: Schematic View of Modelling Transverse Loads at Top and Bottom Flange Levels

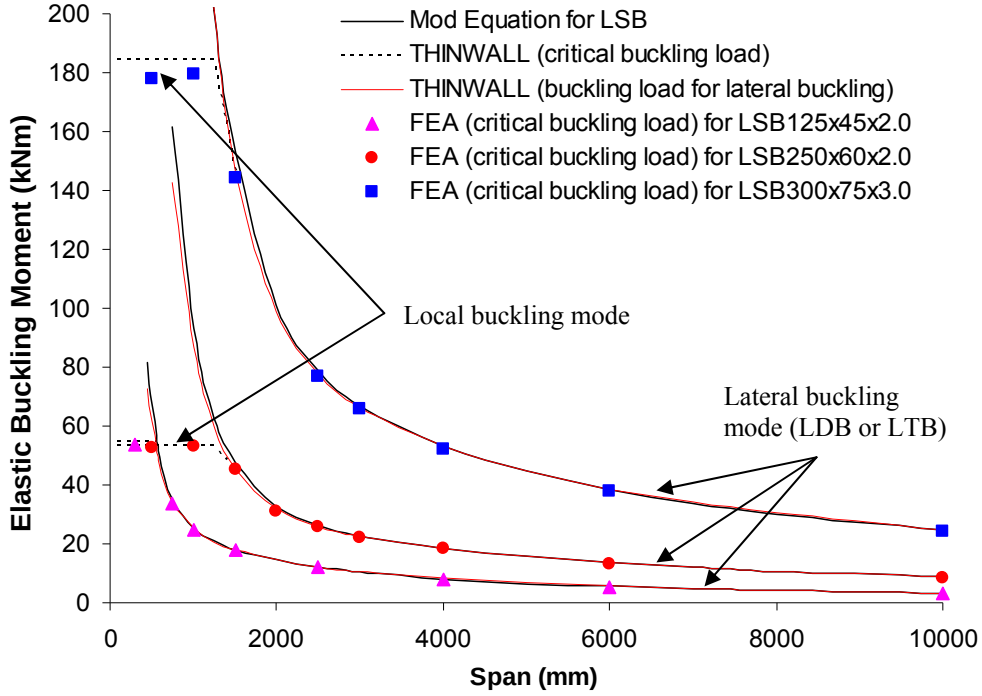

Figure 8: Comparison of Elastic Buckling Moments vs. Span from Finite Element Analysis, THINWALL and the M_{od} Equation for LSBs

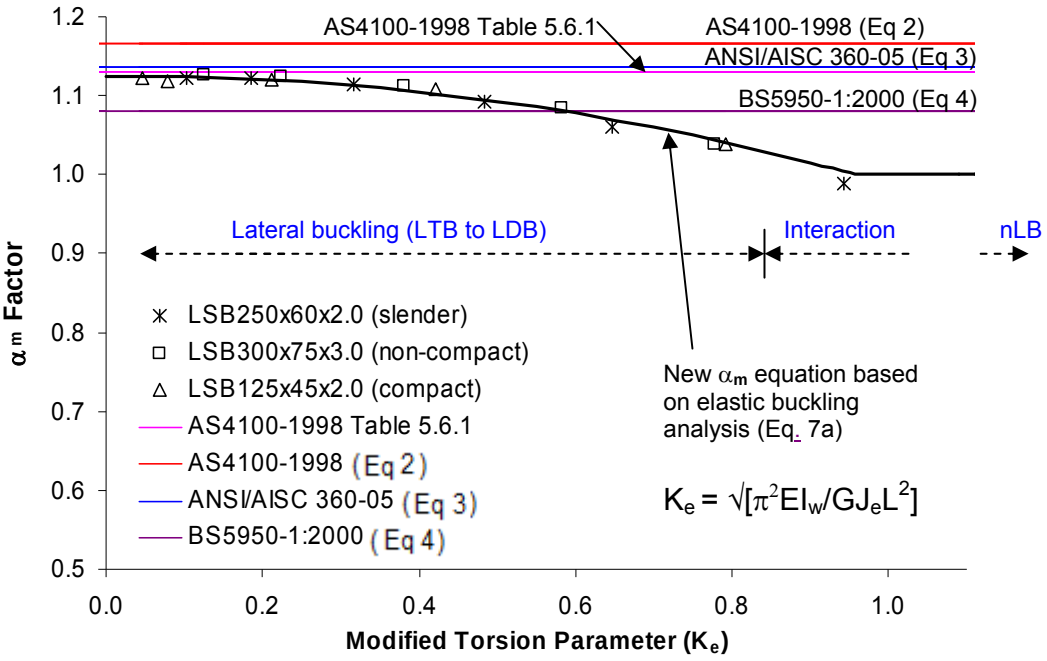

Figure 9: α_m Factors for the UDL Case based on Elastic Buckling Analyses

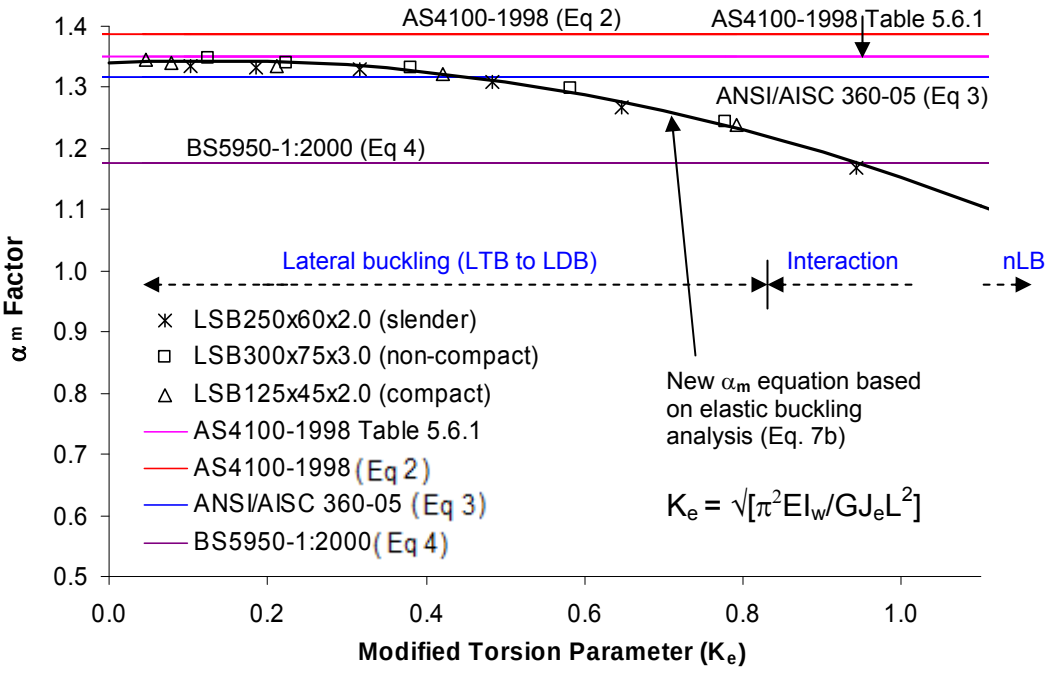

Figure 10: α_m Factors for the PL Case based on Elastic Buckling Analyses

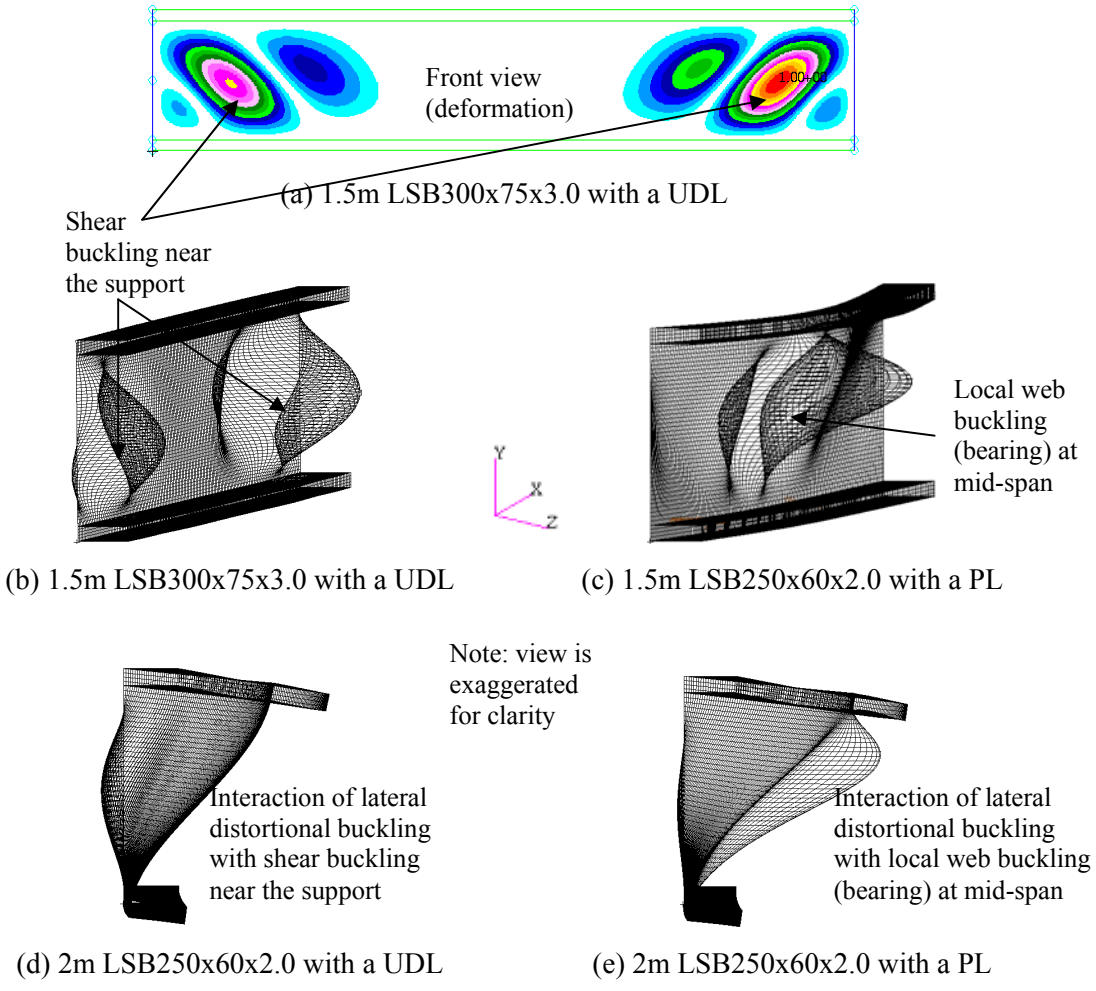

Figure 11: Other Critical Non-lateral Buckling Modes

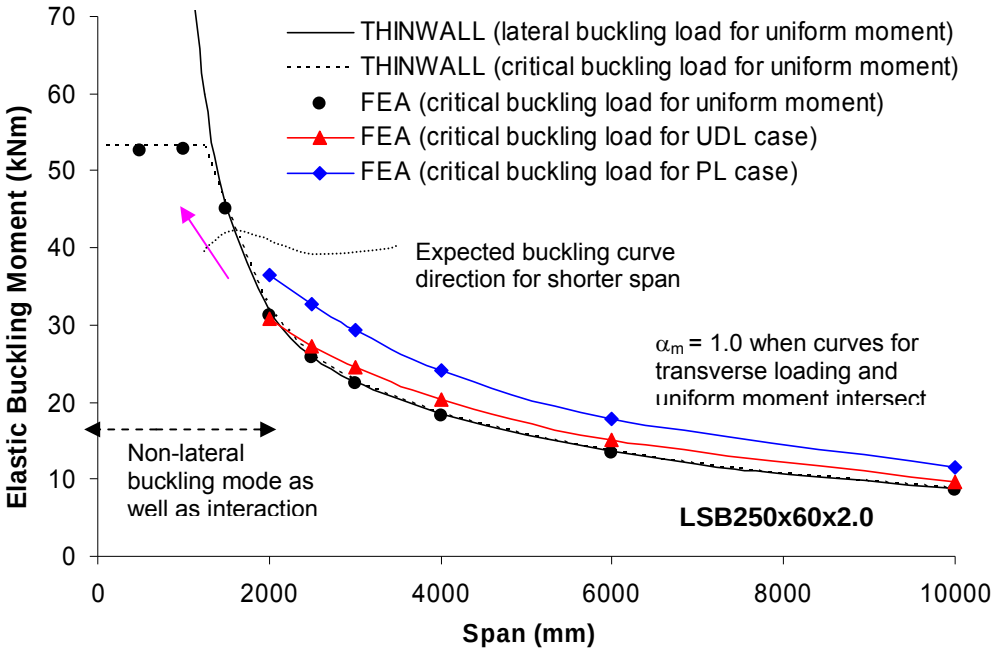

Figure 12: Comparison of Typical Elastic Lateral Buckling Moment versus Span curves for Transverse Loads (UDL and PL) and Uniform Moment Cases

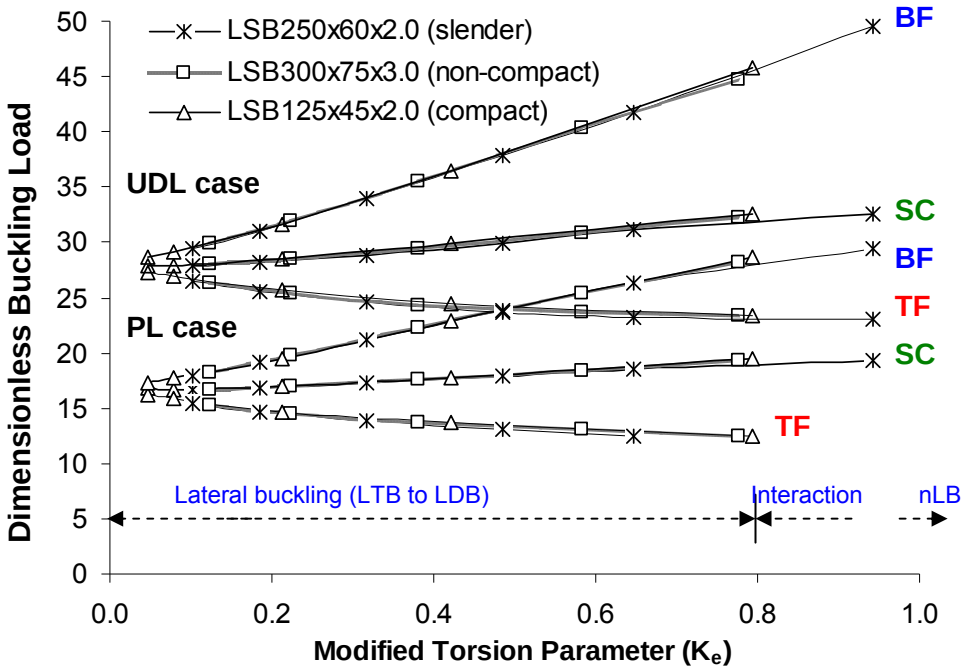

Figure 13: Load Height Effects (Top Flange and Bottom Flange Levels) for Simply Supported LSBs based on Elastic Buckling Analyses

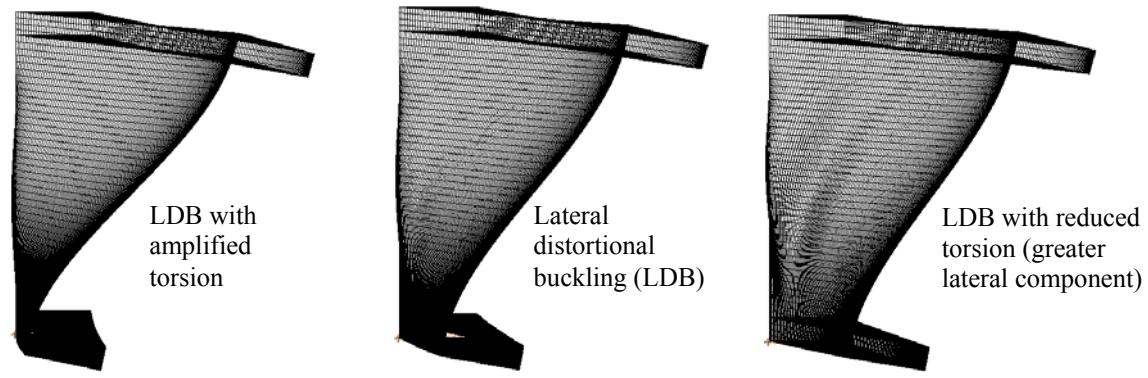

Figure 14: Load Height Effects on the Lateral Distortional Buckling Mode (2.5m LSB250x60x20 Subjected to a UDL)

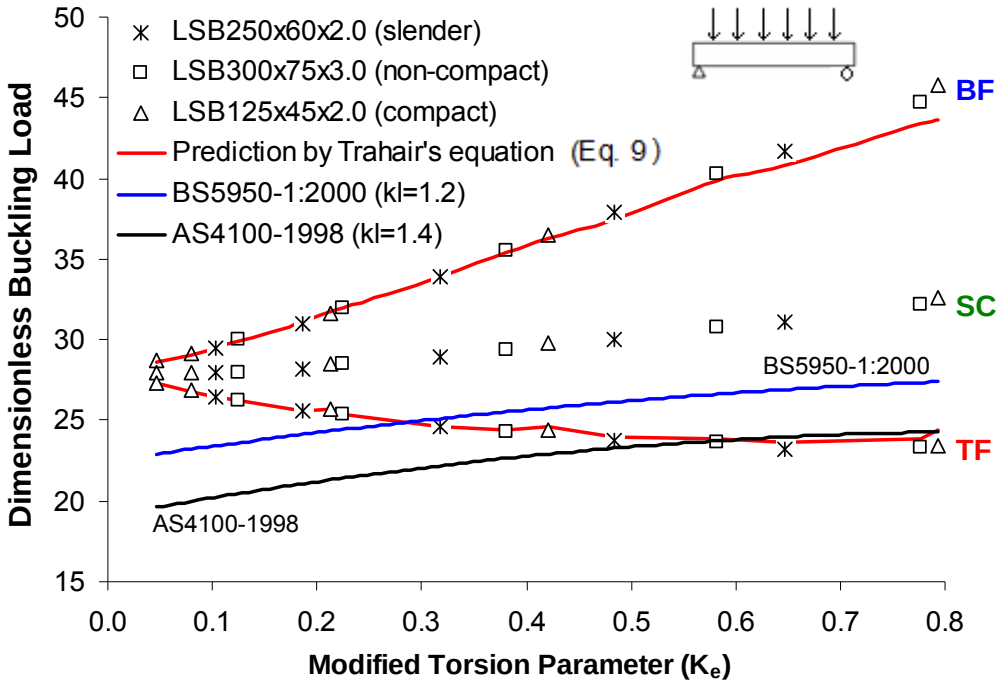

Figure 15: Comparison with Current Design Methods in Predicting the Lateral Buckling Strength of Simply Supported LSBs Subjected to Load Height Effects (UDL Case)

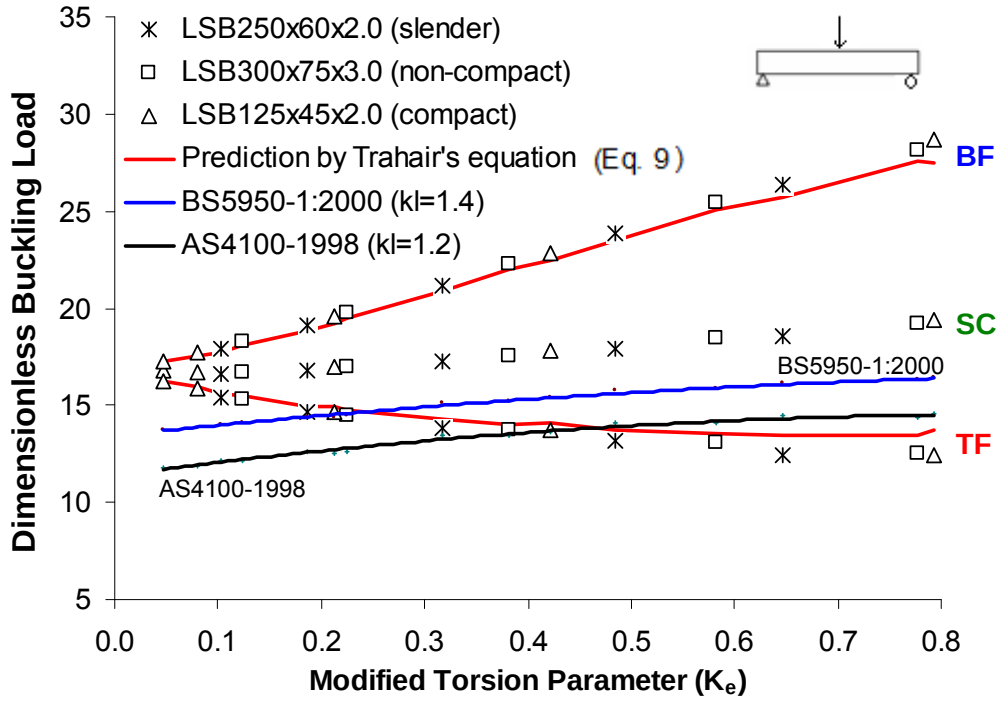

Figure 16: Comparison with Current Design Methods in Predicting the Lateral Buckling Strength of Simply Supported LSBs Subjected to Load Height Effects (PL Case)

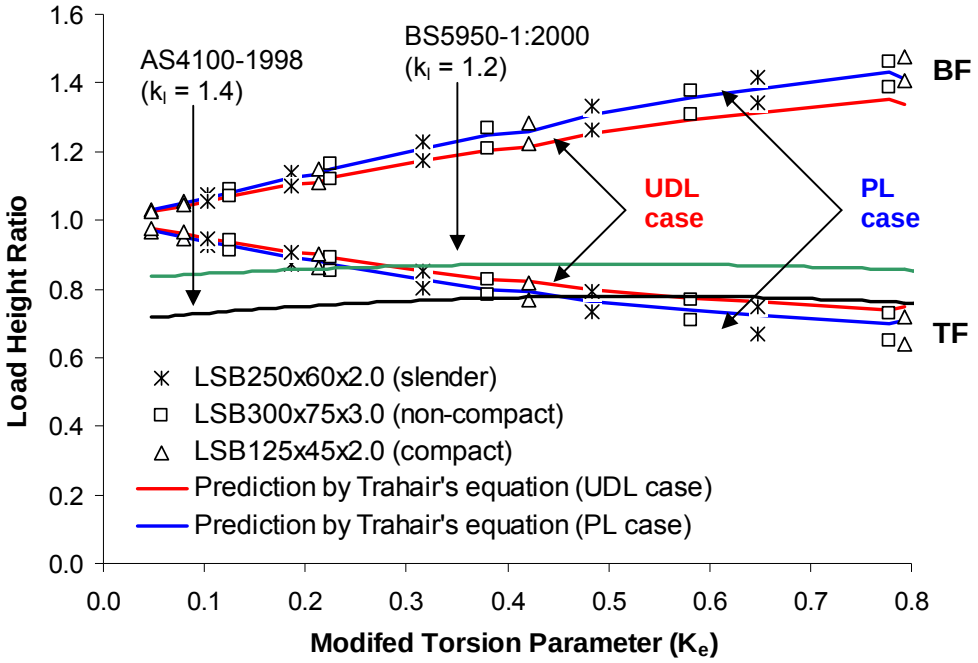

Figure 17: Comparison of Load Height Ratios

Table 1: Elastic Lateral Buckling Moments of Simply Supported LSBs Subjected to a Uniformly Distributed Load (UDL)

LSB d x b_f x t (mm)	Span (mm)	FEA Buckling Moment (M_{od-non}) (kNm)	Mode	α_m Factor	Current α_m Factors: AS4100 Table 5.6.1	AS4100 Eq.2	AISC Eq.3	BS5950.1 Eq.4
125 x 45 x 2.0 LSB	750	*29.76*	***LB***	-	1.13	1.17	1.14	1.08
	1000	25.83	LDB$^+$	1.039	1.13	1.17	1.14	1.08
	1500	19.76	LDB	1.108	1.13	1.17	1.14	1.08
	2500	13.48	LDB	1.121	1.13	1.17	1.14	1.08
	4000	8.98	LDB*	1.122	1.13	1.17	1.14	1.08
	6000	6.12	LTB	1.119	1.13	1.17	1.14	1.08
	10000	3.74	LTB	1.122	1.13	1.17	1.14	1.08
250 x 60 x 2.0 LSB	1500	*29.62*	***nLB***	-	1.13	1.17	1.14	1.08
	2000	30.80	LDB$^+$	0.988	1.13	1.17	1.14	1.08
	2500	27.34	LDB	1.061	1.13	1.17	1.14	1.08
	3000	24.47	LDB	1.092	1.13	1.17	1.14	1.08
	4000	20.28	LDB	1.115	1.13	1.17	1.14	1.08
	6000	14.99	LDB*	1.121	1.13	1.17	1.14	1.08
	10000	9.65	LTB	1.122	1.13	1.17	1.14	1.08
300 x 75 x 3.0 LSB	1500	*96.53*	***nLB***	-	1.13	1.17	1.14	1.08
	2500	79.91	LDB$^+$	1.038	1.13	1.17	1.14	1.08
	3000	70.97	LDB	1.084	1.13	1.17	1.14	1.08
	4000	58.08	LDB	1.113	1.13	1.17	1.14	1.08
	6000	42.55	LDB*	1.125	1.13	1.17	1.14	1.08
	10000	27.15	LTB	1.126	1.13	1.17	1.14	1.08

LDB Lateral distortional buckling mode with negligible web distortion*

LDB$^+$ Lateral distortional buckling mode with shear buckling near the supports (interaction)

nLB *Non-lateral buckling mode (shear buckling near the supports) that precedes LDB*

Table 2: Elastic Lateral Buckling Moments of Simply Supported LSBs Subjected to a Mid-span Point Load (PL)

LSB d x b_f x t (mm)	Span (mm)	FEA Buckling Moment (M_{od-non}) (kNm)	Mode	α_m Factor	Current α_m Factors: AS4100 Table 5.6.1	AS4100 Eq.2	AISC Eq.3	BS5950 Eq.4
125 x 45 x 2.0 LSB	750	*36.41*	***nLB***	-	1.35	1.39	1.32	1.18
	1000	30.79	LDB$^+$	1.239	1.35	1.39	1.32	1.18
	1500	23.58	LDB	1.323	1.35	1.39	1.32	1.18
	2500	16.04	LDB	1.334	1.35	1.39	1.32	1.18
	4000	10.69	LDB*	1.337	1.35	1.39	1.32	1.18
	6000	7.34	LTB	1.341	1.35	1.39	1.32	1.18
	10000	4.48	LTB	1.345	1.35	1.39	1.32	1.18
250 x 60 x 2.0 LSB	1500	*34.17*	***nLB***	-	1.35	1.39	1.32	1.18
	2000	36.41	LDB$^+$	1.168	1.35	1.39	1.32	1.18
	2500	32.68	LDB	1.269	1.35	1.39	1.32	1.18
	3000	29.27	LDB	1.309	1.35	1.39	1.32	1.18
	4000	24.20	LDB	1.330	1.35	1.39	1.32	1.18
	6000	17.81	LDB*	1.332	1.35	1.39	1.32	1.18
	10000	11.49	LTB	1.336	1.35	1.39	1.32	1.18
300 x 75 x 3.0 LSB	1500	*116.3*	***nLB***	-	1.35	1.39	1.32	1.18
	2500	95.64	LDB$^+$	1.243	1.35	1.39	1.32	1.18
	3000	84.96	LDB	1.297	1.35	1.39	1.32	1.18
	4000	69.50	LDB	1.332	1.35	1.39	1.32	1.18
	6000	50.72	LDB*	1.341	1.35	1.39	1.32	1.18
	10000	32.51	LTB	1.348	1.35	1.39	1.32	1.18

LDB Lateral distortional buckling mode with negligible web distortion*

LDB$^+$ Lateral distortional buckling mode with web local buckling at mid-span (interaction)

nLB *Non-lateral buckling mode (web local buckling at mid-span) that precedes LDB*

Table 3: Elastic Lateral Buckling Moments of Simply Supported LSBs Subjected to Top Flange (TF) and Bottom Flange (BF) Loading

LSB d x b_f x t (mm)	Span (mm)	General Buckling Mode	For TF case (kNm)		For BF case (kNm)	
			UDL	PL	UDL	PL
125 x 45 x 2.0 LSB	750	***LB***	-	-	-	-
	1000	LDB	18.56(+)	19.64(+)	36.27	45.37
	1500	LDB	16.16	22.67	24.17	37.82
	2500	LDB	12.13	17.29	14.98	23.08
	4000	LDB*	8.44	7.65	9.55	9.09
	6000	LTB	5.90	8.67	6.39	9.69
	10000	LTB	3.65	5.42	3.83	5.78
250 x 60 x 2.0 LSB	1500	***nLB***	-	-	-	-
	2000	LDB	21.72(+)	20.25(***nLB***)	46.83(+)	55.48(+)
	2500	LDB	20.44	21.87(+)	36.71	46.33
	3000	LDB	19.35	21.47	30.97	38.99
	4000	LDB	17.25	19.47	23.81	29.74
	6000	LDB*	13.59	15.53	16.47	20.30
	10000	LTB	9.13	10.63	10.19	12.38
300 x 75 x 3.0 LSB	1500	***nLB***	-	-	-	-
	2500	LDB	57.99(+)	62.06(+)	110.95	139.76
	3000	LDB	54.36	60.23	92.87	117.15
	4000	LDB	48.14	54.24	70.22	88.03
	6000	LDB*	37.94	43.26	47.74	59.05
	10000	LTB	25.50	29.57	29.10	35.77

LDB Lateral distortional buckling mode with negligible web distortion*

(+) Lateral distortional buckling mode with shear buckling or local web buckling (interaction)

nLB *Non-lateral buckling mode (shear buckling or local web buckling) that precedes LDB*